



Published in final edited form as:

J Control Release. 2018 September 28; 286: 315–325. doi:10.1016/j.jconrel.2018.08.010.

Transcutaneously refillable nanofluidic implant achieves sustained level of tenofovir diphosphate for HIV pre-exposure prophylaxis

Corrine Ying Xuan Chua¹, Priya Jain¹, Andrea Ballerini^{1,2}, Giacomo Bruno³, R. Lyle Hood¹, Manas Gupte⁴, Song Gao⁴, Nicola Di Trani¹, Antonia Susnjar¹, Kathryn Shelton⁵, Lane R. Bushman⁶, Marco Folci¹, Carly S. Filgueira¹, Mark A. Marzinke⁷, Peter L. Anderson⁶, Ming Hu⁴, Pramod Nehete⁵, Roberto C. Arduino⁸, K. Jagannadha Sastry^{5,9}, and Alessandro Grattoni^{1,10,11,*}

¹Department of Nanomedicine, Houston Methodist Research Institute (HMRI), Houston, TX, USA

²Department of Medical Biotechnology and Translational Medicine, University of Milan, Milan, Italy

³Politecnico di Torino, Turin, Italy ⁴Department of Pharmacological and Pharmaceutical Sciences, University of Houston College of Pharmacy, Houston, Texas ⁵Department of Veterinary Sciences, University of Texas MD Anderson Cancer Center, Houston, Texas ⁶Department of Pharmaceutical Sciences, Skaggs School of Pharmacy and Pharmaceutical Sciences, University of Colorado-Anschutz Medical Campus, Aurora, Colorado ⁷Departments of Pathology and Medicine, Johns Hopkins University School of Medicine, Baltimore, Maryland ⁸Division of Infectious Diseases, Department of Internal Medicine, McGovern Medical School at The University of Texas Health Science Center at Houston, Texas ⁹Department of Immunology, University of Texas MD Anderson Cancer Center, Houston, Texas ¹⁰Department of Surgery, Houston Methodist Research Institute (HMRI), Houston, TX, USA ¹¹Department of Radiation Oncology, Houston Methodist Research Institute (HMRI), Houston, TX, USA.

Abstract

Pre-exposure prophylaxis (PrEP) with antiretroviral (ARV) drugs are effective at preventing human immunodeficiency virus (HIV) transmission. However, implementation of PrEP presents significant challenges due to poor user adherence, low accessibility to ARVs and multiple routes

*Corresponding author. agrattoni@houstonmethodist.org.

Author contributions

CCYX coordinated the second animal study, prepared the figures and manuscript. PJ performed *in vitro* HPLC analysis, NDI assembly and helped with the second animal study. PJ and RLH coordinated the pilot study. RLH, GB and AG designed the NDIs. AG and RCA conceived the study. AB, RLH, and AG contributed to the experimental design. CCYX, AB, and AG analyzed the data. MG, MH provided the FTC nanoformulation while GS provided residual drug analysis via LC-MS/MS. KS performed the animal experiment, including device implantation and transcutaneous refilling. PN processed the samples collected from the animals. PLA and LRB analyzed PBMCs and rectal mononuclear cells. MAM analyzed plasma, tissues and cervicovaginal fluid samples. MF performed the histological analyses. The manuscript was revised by AB, CSF, KS, LB, MAM, PLA, PN, RCA, KJS and AG.

Conflict of interest

AG discloses a financial interest in NanoMedical Systems, Inc. PLA receives grants and contract work from Gilead Sciences, paid to his institution. All other authors declare no conflict of interest.

Publisher's Disclaimer: This is a PDF file of an unedited manuscript that has been accepted for publication. As a service to our customers we are providing this early version of the manuscript. The manuscript will undergo copyediting, typesetting, and review of the resulting proof before it is published in its final citable form. Please note that during the production process errors may be discovered which could affect the content, and all legal disclaimers that apply to the journal pertain.

of HIV exposure. To address these challenges, we developed the nanochannel delivery implant (NDI), a subcutaneously implantable device for sustained and constant delivery of tenofovir alafenamide (TAF) and emtricitabine (FTC) for HIV PrEP. Unlike existing drug delivery platforms with finite depots, the NDI incorporates ports allowing for transcutaneous refilling upon drug exhaustion. NDI-mediated drug delivery in rhesus macaques resulted in sustained release of both TAF and FTC for 83 days, as indicated by concentrations of TAF, FTC and their respectively metabolites in plasma, PBMCs, rectal mononuclear cells and tissues associated with HIV transmission. Notably, clinically relevant preventative levels of tenofovir diphosphate were achieved as early as 3 days after NDI implantation. We also demonstrated the feasibility of transcutaneous drug refilling to extend the duration of PrEP drug delivery in NHPs. Overall, the NDI represents an innovative strategy for long-term HIV PrEP administration in both developed and developing countries.

One Sentence Summary:

Transcutaneously refillable nanofluidic implant achieves sustained level of tenofovir diphosphate for HIV pre-exposure prophylaxis

1. INTRODUCTION

Human immunodeficiency virus (HIV) remains a global health problem with approximately 36.7 million people living with the virus, and an estimated 2.1 million new cases per year (1). According to the Prevention gap report, efforts to decrease new adult HIV infections are substantially off track (2). The decline in new HIV infections has been stagnant since 2010, and there is an alarming estimate of 57% increase in new infections in certain regions. In order to avoid resurgence of HIV incidence rates, concerted global efforts are focused on HIV prevention strategies. Of note, biomedical intervention using co-formulated tenofovir (TFV) disoproxil fumarate (TDF) and emtricitabine (FTC) antiretroviral ARV drugs as pre-exposure prophylaxis (PrEP) is highly effective at preventing HIV transmission when taken daily as prescribed (3–8). However, according to clinical studies, the efficacy of PrEP is limited by user adherence to the regimen (9). Strict adherence to PrEP regimen of at least 4 doses a week reduced HIV transmission risk by up to 96%, whereas lower adherence resulted in preventative efficacy of only 42% (3–5, 10, 11). These clinical studies highlight the importance of user adherence for maximal PrEP efficacy. The target is to have 3 million high risk individuals on PrEP by 2020, however according to UNAID 2017, as of June 2017 the number of people on PrEP between 2012 and early 2017 has been estimated at nearly 250,000, whereby 220,000 were from the United States of America. Given that PrEP coverage is only at less than 10% of the 2020 target, considerable effort is needed to extend PrEP provision and implementation (12).

HIV PrEP modalities include local or systemic interventions that are administered on a fixed schedule or exposure-driven manner. Local approaches such as topical gels (13–15) and self-inserted vaginal rings (16–20) that contain ARVs have shown modest success at preventing HIV in comparison to once-daily oral FTC/TDF pill (21). A systemic intervention approach offers the advantage of simultaneous protection from infection in multiple compartments of exposure (22). Accordingly, extensive research is focused on developing long-acting ARV

strategies including long-acting (LA) injectables or implants, which reduce dosing frequency to improve PrEP implementation and adherence. Investigational LA injectables for PrEP, such as cabotegravir and rilpivirine, are administered at 8–12 weeks interval through intramuscular injection. Plasma cabotegravir levels were detectable up to 52 weeks after one injection, suggesting the potential effectiveness of LA injectables for PrEP. However, once injected there is no way to remove the drug should the individual develop drug-related adverse events. While long-acting injectables eliminate the need for once daily ARV pills, the issue of adherence to injection schedule remains. An alternative LA strategy being explored is subcutaneous implants for sustained ARV delivery, with encouraging results in *in vitro* and *in vivo* studies in beagle dogs (23, 24). Further, the Medici Drug Delivery System™ developed by Intarcia Therapeutics, which is a matchstick-sized subcutaneous implant utilizing an osmotic mini-pump for drug delivery, is currently under investigation for HIV PrEP. While these sustained drug delivery depots are a promising systemic PrEP strategy and can be removed if the individual develops side effects, they require explantation and re-implantation procedures upon drug exhaustion.

To overcome adherence challenges and improve on current PrEP delivery strategies, we present the nanochannel delivery implant (NDI), a subcutaneous implant for sustained systemic ARV delivery with a transcutaneous refillable feature for drug replenishing. The NDI is composed of biocompatible components, including a medical grade titanium drug reservoir, a silicon nanochannel membrane to control drug release and two resealable silicone drug loading ports for transcutaneous refilling. Sustained and constant drug delivery is achieved via diffusion through the nanochannel membrane, obviating the need for pumps, catheters, or clinician intervention. In this study, we investigated the sustained release of FTC and tenofovir alafenamide (TAF) via the NDI in *in vitro* studies and in rhesus macaques. Daily FTC (200 mg)/TAF (25 mg) single tablet combination is United States Food and Drug Administration (FDA) approved for HIV treatment. The safety and efficacy of FTC/TAF is currently being evaluated for HIV PrEP (NCT02842086). Unlike TDF, TAF remains stable in the plasma where it can diffuse into cells and conversion into TFV primarily occurs intracellularly in targeted lymphoid cells, followed by phosphorylation into the active metabolite TFV-diphosphate (TFV-DP)(25). Thus, TAF administration results in low plasma TFV levels and high intracellular levels of TFV-DP, effectively minimizing kidney and bone-related side effects while maximizing drug potency (26). Similarly, FTC is phosphorylated intracellularly into active metabolite, FTC-triphosphate (FTC-TP).

Here, we first conducted *in vitro* analyses of TAF and FTC release from the NDI to assess drug release rate. We next performed a pilot study in a rhesus macaque to gain insight into achievable target dose of ARV delivery via the NDI and to establish the efficacy of the NDI to sustainably deliver ARV. Next, we expanded the study to three rhesus macaques to evaluate sustained ARV delivery over a period of 3 months and establish proof of concept for transcutaneous refilling. We evaluated the pharmacokinetics of TAF and FTC, and their respective drug metabolites, in plasma, PBMCs, and anatomic sites associated with HIV transmission. Based on a *post hoc* analysis of IPREX and other clinical studies, TFV-DP concentration of 40 fmol/10⁶ cells for freshly lysed peripheral blood mononuclear cells (PBMCs) or 16 fmol/10⁶ cells for viably cryopreserved PBMCs was associated with 90% reduction in HIV infection risk (EC₉₀) in men who have sex with men (MSM) (11, 27). As

for FTC-TP, the EC₉₀ is 5000 – 6000 fmol/10⁶ cells for freshly lysed PBMCs and 3700 fmol/10⁶ cells for viably cryopreserved PBMCs in MSM. We primarily focused on the levels of active drug metabolites, TFV-DP and FTC-TP in PBMCs in our studies as an indicator of effective *in vivo* drug delivery from the NDI. Finally, we evaluated the feasibility of transcutaneous refilling to extend the duration of drug release without device explantation.

2. MATERIALS AND METHODS

2.1. Study design

This study was designed to investigate the efficacy of HIV PrEP drug release from subcutaneously implanted devices in rhesus macaques. For initial feasibility assessment, a short-term pilot study of 22 days was conducted using one animal. This animal was implanted with three nanofluidic drug delivery devices, each releasing PBS (control), TAF, or FTC, to determine achievable *in vivo* drug concentration over 3 weeks. The second study was expanded to three animals with an extended study duration of 83 days. In this second study, each animal was implanted with two nanofluidic devices, each releasing either TAF or FTC. The primary objective of the second study was to evaluate long term *in vivo* drug delivery via the nanofluidic device. The secondary objective was to assess an additional parameter of transcutaneous drug refilling to replenish reservoir and maintain constant drug release. Blood draws and swabs were performed at pre-determined time points as specified in figures. HPLC was performed to analyze drug concentration in *in vitro* experiments whereas LC-MS/MS was performed to analyze drug concentration in *in vivo* experiments. Data analyses were performed as described.

2.2. Materials.

Tenofovir alafenamide (TAF) and emtricitabine (FTC) were kindly provided by Gilead Sciences, Inc. (Foster City, CA).

2.3. Nanochannel Delivery Implant (NDI)

Silicon microfabricated membranes presenting 20 and 250 nm nanochannels were used (28, 29). Respectively, these membranes house 340,252 and 1,900,800 slit-nanochannels parallel to the membrane surface, densely organized in square arrays and connected to the membrane inlet and outlet via arrays of microchannels (fig. 1 A). All nanochannels were obtained in a bioinert and biocompatible TaN coated structure with strict dimensional tolerances (~4.4 Å) via a sacrificial layer technique (29). The nanochannel membranes were immersed in 100% isopropanol to promote wetting of all channels and then rinsed with Millipore water prior to use (29, 30). Implantable medical-grade titanium reservoirs and silicon plugs were autoclaved and maintained in a sterile field for assembly and loading. For the pilot study, we mounted 20 nm nanochannel membranes along with silicone septa each onto a reservoir (16.6 mm x 16.6 mm) with UV epoxy (EPOTEK # OG116–31). The devices were empty or loaded with either powder FTC (69.1 mg) or TAF (72.9 mg) and sealed with silicone (NUSIL Technology # MED3–4213). For the empty device, phosphate-buffered saline (PBS) was injected through the septum with a 30 gauge needle. For the drug-filled devices, PBS was injected through the loading port with a 30 gauge needle while a needle in the venting port was maintained to vent out excess air indicating the membrane had been fully

primed (fig. 1G). For the transcutaneous refilling study, NDI with reservoirs of either approximately 6 ml or 3g (FTC; 43 mm x 28.5 mm x 8.7 mm; 250 nm nanochannel) and 550 μ l or 200 mg (TAF; 5 mm x 20 mm x 12.3 mm; 20 nm nanochannel) were fabricated with implantable medical-grade titanium (Ti6Al4V), loaded with powder drug, and sealed with UV epoxy (EPOTEK # OG116-31). Drug loading ports were closed with silicon septum and the edges sealed with UV epoxy. The membranes were primed with PBS as in the pilot study.

2.4. In vitro release studies.

Cylindrical implants were loaded with either 2.6 mg of TAF (n = 4) or 2.8 mg of FTC (n = 4) and placed in sink solution of 2.5 ml 1X PBS in a cuvette for ultraviolet/visible (UV/Vis) spectroscopy measurements. In vitro analysis was performed with a custom robotic carousel interfaced with a UV/Vis spectrophotometer (Cary 50, Agilent Technologies) (31) by collecting absorbance measurements of the sink solution ($\lambda=260$ nm for TAF and 280 nm for FTC) every 4 minutes 45 seconds with continuous magnetic stirring of sink solution. This setup was adopted to minimize the experimental error and substantially increase the number of collected data points.

2.5. HPLC measurement of residual drug analysis from implant.

Residual drug solution from used implants was extracted from the silicone plugs on the devices using a 20 G needle before the device was opened and left in 100% methanol overnight. TAF residual was brought up to 10 ml in 100% methanol using a volumetric flask while FTC was brought up to 25 ml. The concentrations of TAF and FTC were measured by adapting a previously described method for HPLC with UV detection (Hitachi Chromaster) (24). A Restek (Bellefonte, PA, USA) Ultra-biphenyl column (2.1 \times 100 mm, 5 μ m) controlled at 30°C was used as the stationary phase. A solution of 1% acetic acid, 3% acetonitrile, and water was used as mobile phase preparation A while acetonitrile was used as mobile phase B to follow the gradient program listed in Supplemental Table 1 with a flow rate of 0.50 ml/min and a detection wavelength of 260 nm. Injection volume was 20 μ l, and total run time was 14 min. The retention times for TAF and FTC were 9 minutes and 4.5 minutes, respectively.

2.6. Animals.

The pharmacokinetics and preliminary safety animal study were conducted at the AAALAC-I accredited Michale E. Keeling Center for Comparative Medicine and Research, The University of Texas MD Anderson Cancer Center (UTMDACC), Bastrop, TX. All animal experiments were carried out according to the provisions of the Animal Welfare Act, PHS Animal Welfare Policy, and the principles of the NIH Guide for the Care and Use of Laboratory Animals. All procedures were approved by the Institutional Animal Care and Use Committee at UTMDACC. Rhesus macaques (*Macaca mulatta*; n= 4) of 2, 14, 15 and 19 years were used in the study. Animals were housed under standard conditions, had *ad libitum* access to water and a standard laboratory diet.

2.7. Implantation procedure.

The anesthetized animal was placed in ventral recumbency and the surgical site aseptically prepared. A skin incision was made parallel to the vertebral column in the dorsal scapular region. Within the incision line, a subcutaneous pocket large enough to accommodate the size of the implant was made by blunt dissection for placement of the implant. The device was placed in the subcutaneous pocket with the drug-eluting side facing the dermis and the drug refilling ports facing up towards the epidermis. The skin and subcutaneous incisions were closed with absorbable monofilament sutures.

2.8. Blood collection, plasma and PBMCs sample preparation.

Blood (7 ml) was collected in EDTA coated vacutainer tubes (Becton, Dickinson and Company, Franklin Lakes, NJ) twice weekly for the first month and once weekly thereafter. Plasma was separated from blood by centrifugation at $1200 \times g$ for 10 minutes (min) at 4°C and stored at -80°C till further use. Remaining blood was used for PBMCs separation by the standard Ficoll-Hypaque (SIGMA, Histopaque-1077), centrifugation. Cell viability was $>95\%$. After counting cells, cells were pelleted by centrifugation at $400 \times g$ at 4°C for 10 min and resuspended in $500 \mu\text{l}$ of cold 70% methanol/30% water, and stored at -80°C until drug concentration analysis.

2.9. Rectal biopsy and rectal mononuclear cell isolation.

Rectal biopsies were performed once a month. Rectal biopsies were collected in 30 ml PBS, washed once with 30 – 40 ml of PBS, centrifuged and resuspended in 25 ml PBS containing 0.5 mg/ml collagenase (C2139 type VIII) and 15 $\mu\text{g}/\text{ml}$ DNaseI and digested at 37°C for 30 – 60 min in incubator shaker (300 rpm). After digestion, cell suspension was passed through a $70 \mu\text{m}$ cell strainer twice. Cell viability was $>95\%$. The cell pellet was stored at -80°C in 70% methanol until drug concentration analysis.

2.10. Quantification of TAF, TFV and FTC plasma, cervicovaginal fluid and tissue concentrations

TFV, FTC, and TFV-DP concentrations in plasma, tissue, cervicovaginal fluid (CVF), and rectal fluid (RF) were quantified using previously described liquid chromatographic-tandem mass spectrometric (LC-MS/MS) analysis (32, 33). Plasma TAF quantification of three-monkey study was performed using a method validation in accordance with FDA Bioanalytical guidelines. Briefly, 0.1 ml of plasma was subjected to solid phase extraction; analytes were ultimately separated via liquid chromatography using a Waters Acquity UPLC system interfaced with a API5000 mass analyzers (SCIEX, Foster City, CA). Chromatographic separation occurred using a Zorbax Eclipse Plus C18 Narrow Bore RR, $2.1 \times 50 \text{ mm}$, $3.5 \mu\text{m}$ column (Agilent, Wilmington, DE). TAF was quantified using $^{13}\text{C}_5$ -TFV as an internal standard; transitions for TAF and the internal standard were m/z $477.3 \rightarrow 176.0$ and m/z $293.1 \rightarrow 181.1$, respectively. TFV and FTC concentrations in oral fluid (OF) were quantified from a RF standard curve using a modified version of the aforementioned LC-MS/MS method. Assay lower limits of quantification (LLOQ) were as follows: Plasma TFV and FTC: 0.31 ng/mL, TAF: 0.03 ng/ml; CVF, RF, and OR: TFV, 5 ng/ml; FTC, 20 ng/ml; tissue TFV: 0.05 ng/sample, TFV-DP: 50 fmol/sample; FTC: 0.25 ng/

sample. Tissue concentrations were normalized to ng/mg or fmol/mg based on the weight of tissue analyzed. Median tissue weights used for analysis were 35.6 mg. Plasma and swabs from one-monkey pilot study were analyzed for TAF, TFV and FTC concentrations using Waters Xevo TQ-S mass spectrometer coupled to Waters Acquity UPLC with analytical column Phenomenex Synergi Fusion 4 μ m, 2 \times 150 mm at the Pharmaceutical Science Facility of the University of Texas at MD Anderson Cancer Center.

2.11. Quantification of PBMC TFV-DP and FTC-TP concentrations.

TFV-DP and FTC-TP were quantified in freshly lysed PBMCs using a validated LC-MS/MS assay, as previously described (34). The quantifiable linear range for TFV-DP was 2.5–2000 fmol per sample and for FTC-TP was 0.1–200 pmol per sample. Approximately 2 million total cells were used for analysis, and results were reported as fmol per million PBMCs.

2.12. Quantification of rectal mononuclear cells TFV-DP and FTC-TP concentrations.

TFV-DP and FTC-TP concentrations in freshly lysed rectal mononuclear cells were assayed with a validated LC-MS/MS method, as previously described (34, 35). The lower limit of quantification (LOQ) was 2.5 fmol/sample for TFV-DP and 0.1 pmol/sample for FTC-TP.

2.13. FTC nanosuspension formulation.

FTC nanoformulation was prepared using the wet milling technique. Glass beads of three diameters (0.5 μ m - 0.75 μ m, 0.75 μ m - 1 μ m and 1 μ m - 1.3 μ m) were added to a glass vial in 1:1:1 ratio. 10% w/v aqueous solution of Polysorbate 80 and 10% w/v aqueous solution of Pluronic F108 were prepared. Polysorbate 80 and Pluronic F108 were used as a hydrophilic nonionic surfactant to maintain colloidal stability. FTC was weighed and added to the vial containing the glass beads such that each ml of the suspending media contained 1 g of FTC. Equal volumes of 10% polysorbate 80 and 10% Pluronic F108 were further added to the vial. The mixture was further diluted two times with deionized (DI) water and stirred using magnetic stirrers for 36 hours at 1600 rpm. FTC nanosuspensions after being stirred for 36 hours were diluted using DI water to obtain a final concentration of 0.4 g/ml. The size and zeta potential were assessed to determine stability via dynamic light scattering (DLS) using Zetasizer Nano ZS (Malvern, Worcestershire, UK) whereby the size ranged from 256 to 387 nm and zeta potential of -37 to -48 mV over several weeks.

2.14. Transcutaneous refilling procedure

Anesthetized animal was placed in ventral recumbency on the surgical table and dorsum area was prepared using chlorhexidine scrub and solution. Palpable ports on the NDI enabled accurate placement of a venting syringe in the venting port, while solution-filled syringe was placed in the adjacent port. Drug residue was extracted from the venting port, creating a negative pressure in the reservoir, which produced a suction effect to facilitate washing or refilling from the drug loading port. Residual TAF was flushed out using 100% ethanol three times, followed by three flushes with 50% ethanol. TAF was solubilized in 50% ethanol in 1 X PBS (230 mg/ml) and used to replenish the reservoir with three consecutive injections of TAF solution (550 μ l each). Residual FTC was flushed out with sterile water five times, followed by three consecutive injections of FTC nanoformulation solution (0.4 mg/ml; 6 ml

each) into the reservoir. All solutions flushed out from the device were collected and analyzed via LC-MS/MS. NDI-FTC in all three NHPs were transcutaneously refilled. For the 2-year old macaque, NDI-TAF refilling occurred transcutaneously, while for the two older macaques (15 and 19 years old) that developed age-related wound-healing issues around the implant site, refilling was performed *ex vivo* prior to device re-implantation.

2.15. Ultrasound analysis

SonoSite 180 Plus ultrasound device (SonoSite, Bothell, WA) was used for ultrasound analysis of NDI subcutaneously implanted in a cadaveric Yorkshire pig (70 kg). Ultrasound transmission gel, Aquasonic 100 (Fairfield, NJ) was used during ultrasound analysis.

2.16. Histological analysis

Tissues were fixed in 10% buffered formalin, embedded in paraffin, cut into 5 μm sections and stained with hematoxylin & eosin (H&E) at the Research Pathology Core of Houston Methodist Research Institute (HMRI), Houston, TX, USA.

2.17. Statistical analysis

GraphPad Prism 7 (version 7.0a; GraphPad Software, Inc., La Jolla, CA) was used to plot all graphs and perform statistical analyses. Data are represented as mean \pm SEM or median and interquartile range (IQR) between the first (25th percentile) and third (75th percentile) quartiles.

3. RESULTS

3.1. Nanochannel delivery implant

We designed the NDI as a transcutaneously refillable drug-eluting implant for TAF and FTC release (fig. 1). The NDI utilizes a silicon nanochannel membrane to control drug diffusion from its reservoir. Nanochannels are densely packed, geometrically organized in arrays and connected to the membrane surface via inlet and outlet microchannels (fig. 1A - C). Although drugs are ultimately released through microchannels, nanochannels represent the bottleneck in the transmembrane transport, and their dimension and number control the rate of release. Drug delivery is driven by a difference in concentration and its rate regulated by electrostatic and steric hindrance effects in nanoconfinement (28, 36–38). Specifically, at increasing level of confinement, molecules diffusing through nanochannels are subjected to enhanced electrostatic interactions with the channel surfaces. This generates a saturated diffusive transport that is quasi-independent from the concentration gradient (30, 39, 40). As such, sustained and constant drug delivery is achieved without pumps, catheters, or clinician intervention. By adopting a refined sacrificial layer microfabrication technique, silicon membranes with monodisperse 20 and 250 nm *slit*-nanochannels (3 μm in width and 1 μm in length) were achieved with dimensional tolerances of ~ 4.4 Å. This was determined via ImageJ software analysis of TEM micrographs of the channel cross section. A total number of 340,252 and 1,900,800 nanochannels were generated for the 20 and 250 nm membranes, respectively. Membrane degradation testing coupled with atomic force microscopy (AFM) and Energy Dispersive X-ray Spectroscopy (EDX) showed that the TaN/SiC coating provided bioinertness and protected membranes from degradation in PBS under accelerated

conditions (90 °C) over 60 days, as well as at 23 °C over 5 years (fig. 1D-F). Similar surface morphology and roughness were detected by AFM for the 5 year samples as compared to fresh controls (fig. 1D, E). EDX highlighted the same surface elements indicating that the membrane layers underneath the TaN/SiC coating were not exposed by degradation (fig. 1F). These results indicate that the membrane is chemically inert and resilient, as required for refillable drug delivery implants. Further, the NDI incorporates drug-loading ports to allow for transcutaneous drug refilling, which obviates the need for device explantation to replenish drug (fig. 1G). The implantable grade silicone ports were shown to be mechanically robust and self-sealing after piercing with needles. In this context, nitrogen flow testing performed with 15 psi differential pressure after repeated piercing with 25 and 30 gauge needles showed no leakage for >20 and >30 sequential piercing (n=6 for each needle size), respectively. All components of the NDI including the drug reservoir (implantable grade Ti6Al4V titanium and silicone plugs) and the nanochannel membrane (composed of silicon, silicon nitride and silicon carbide (SiC)), have been identified as biocompatible (41–43).

3.2. Pilot in vitro and in vivo study of NDI-ARV

The nanochannel size was selected by accounting for the physicochemical properties of the drug molecules, by adopting an algorithm that we previously developed via experimental release testing of different drugs (28). Additionally, we accounted for the drug formulation, which in this study was chosen to be in powder form with the purpose of maximizing stability and minimizing volume of the NDI. To determine the release rates, *in vitro* TAF and FTC release from NDIs with 20 nm nanochannel membranes were evaluated over 24 hours. Each NDI was filled with either powder TAF (NDI-TAF) or FTC (NDI-FTC). *in vitro* cumulative release profiles exhibited constant release kinetics, whereby TAF (fig. 2A) achieved a cumulative release of 0.21 ± 0.03 mg, while FTC (fig. 2B) reached a cumulative release of 2.67 ± 0.35 mg.

To evaluate preliminary safety and drug delivery efficacy of the NDI, we performed a pilot study where we subcutaneously implanted three NDIs into a rhesus macaque. Each NDI was filled with either powder TAF (NDI-TAF), powder FTC (NDI-FTC), or sterile phosphate buffered saline solution (NDI-PBS), respectively. NDI-TAF and NDI-FTC were implanted for 22 days for drug delivery analysis, whereas NDI-PBS was implanted for 60 days to evaluate long term impact of the subcutaneous implant. To compare the differential drug distribution and accumulation, TAF, TFV and FTC concentrations were measured in plasma and mucosal tissues namely, rectal, urethral and oral swabs. Throughout the 22 days of subcutaneous drug delivery from the NDI, we observed sustained levels of plasma TAF (median 0.10 ng/ml; IQR, 0.07 to 0.2 ng/ml) and FTC (median 12.9 ng/ml; IQR, 9.1 to 19.5 ng/ml), while plasma TFV levels were below the lower limit of quantification (LOQ) (fig. S1A). Rectal, urethral, and oral swabs samples demonstrated varying levels of TAF, TFV, and FTC over a period of 22 days (fig. S1B). Consistent with the TAF metabolic pathway, rectal, urethral and oral samples displayed sustained levels of TFV compared to TAF. In line with literature reports, TFV level (median 0.9 ng/ml; IQR, 0.1 to 1.3 ng/ml) in rectal mucosa was higher than FTC (median 0.06 ng/ml; IQR, 0.03 to 0.3 ng/ml) (44). FTC concentration was lower than TFV in urethral tissue, but higher than TFV in oral samples. Notably, TFV

levels were still detectable on day 30 in rectal, urethral, and oral swab samples after device explantation. Plasma drug levels indicate sustained drug exposure, whereas intracellular drug concentrations are critical for inhibition of viral replication. Intracellular TFV-DP and FTC-TP concentrations in PBMCs were analyzed as a measure of drug delivery efficacy. As early as day 3 after implantation of NDI, TFV-DP concentration in PBMCs reached the preventative target (fig. S2). A median TFV-DP concentration of 40.3 fmol/10⁶ PBMCs (IQR, 23.8 to 56.1 fmol/10⁶ PBMCs) was detected throughout the 22-day study (fig. S2). TFV-DP levels declined on the day of NDI explantation (day 22), and dropped to 4.61 fmol/10⁶ PBMCs on day 30 (fig. S2). Conversely, FTC-TP levels were below the clinically relevant target concentration at a median concentration of 73.1 fmol/10⁶ PBMCs (IQR, 52.3 to 100.3 fmol/10⁶ PBMCs) over the 22-day period and dropped to below LOQ two days after explantation. Residual drug analysis on the implants showed that 54.9% (40.0 mg) of the TAF payload was delivered over the 22-day study whereas 95.2% (65.8 mg) of FTC payload was released *in vivo*, likely due to differences in aqueous solubility of the drugs (fig. S3A, B). These results indicate that larger nanochannel size and number and drug reservoir size would be needed for greater and longer release of FTC. TAF was released from the NDI at an estimated rate of 1.8 mg/day, while FTC was delivered at 3.0 mg/day *in vivo* (fig. S3C). Consistent with previous studies (38, 45), residual drug analysis demonstrated that *in vivo* release rate from the NDI was substantially higher than the *in vitro* release rate. This is particularly evident for TAF, which presents 80% protein binding affinity (46). As such, higher release rates can be attributed to factors such as the enhanced solubilization in physiological conditions in the presence of proteins such as albumin. Albumin and other biological molecules can permeate the implant reservoir and shuttle TAF across the membrane into the body. No adverse skin reactions occurred throughout the duration of the 60-day implantation of NDI-PBS. Histology sections of skin punch biopsies of tissue adjacent to the implanted devices 3 weeks after implantation revealed minimal immune cell infiltration and inflammation (fig. S4A-D).

3.3. Pharmacokinetic profile of TAF, TFV and FTC concentrations in plasma over 70 days

We next sought to extend NDI-facilitated drug release to 90 days *in vivo*. In this study, we utilized an elongated design of the NDIs with larger drug reservoirs, incorporating two loading ports with resealable silicon plugs (one for drug-loading and the other for venting) to allow for transcutaneous refilling upon drug depletion from reservoir (fig 1G). Further, as FTC-TP concentration in PBMCs in our pilot study did not reach preventative target, the new NDI-FTC implant was assembled with a 250 nm nanochannel membrane (as opposed to 20 nm) to facilitate a higher dose release. An FTC *in vitro* release study confirmed ~8-fold enhanced release corresponding to a rate of 21.38 mg/day with the 250 nm nanochannel membrane (fig. S5). The same 20 nm nanochannel membrane as in the pilot study was adopted for NDI-TAF. Next, using these newly designed NDIs, we conducted a study with three rhesus macaques to evaluate NDI-facilitated drug release for approximately 3 months. NDIs were loaded with powder drug, and each animal was subcutaneously implanted with one NDI-TAF and NDI-FTC. Drug delivery efficacy from the NDI was evaluated using the pharmacokinetic profile of TAF, TFV and FTC in plasma, TFV-DP and FTC-TP in PBMCs and rectal mononuclear cells, TFV and FTC in the rectum, cheek pouch, cervix, inguinal lymph node (LN) and cervicovaginal fluid. Over the course of 70 days (pre-transcutaneous

refilling), we observed increasing plasma levels of both TAF (median 0.1 ng/ml; IQR, 0.05 to 0.5 ng/ml) and TFV (median 3.5 ng/ml; IQR, 1.9 to 7.2 ng/ml). Consistent with published report, we detected higher plasma TFV levels relative to TAF, which could be attributed to TAF metabolism to TFV (24). On the contrary, while FTC was detected in the plasma (median 390.3 ng/ml; IQR, 107.1 to 655.7 ng/ml), we observed a declining trend from day 3 to 70 (fig. 3), possible due to its short plasma half-life of 8 to 10 hours (47).

3.4. Pharmacokinetic profile of TFV-DP and FTC-TP in PBMCs and rectal mononuclear cells

The drug concentrations in plasma samples showed efficient release of TAF and FTC from the NDIs. To determine if target preventative concentration was achieved, we analyzed TFV-DP and FTC-TP levels in PBMCs on a weekly basis as a surrogate indicator of drug exhaustion from NDI reservoir, to gauge when to perform transcutaneous refilling (fig. 4). Subcutaneous delivery of TAF and FTC from the NDI resulted in conversion into active intracellular metabolites, TFV-DP and FTC-TP, respectively, at the first sampling time point (day 3 after implantation). TFV-DP levels in PBMCs reached target preventative levels as early as 3 days after implantation, and continued to increase from a mean of 71.7 ± 29.7 to 533.3 ± 198.4 fmol/ 10^6 PBMCs over a period of 70 days (pre-transcutaneous refilling) (fig. 4). This gradual accumulation observed is consistent with the long intracellular half-life of TFV-DP (150 hours), as seen in clinical studies (25, 48). TFV-DP exposure in rectal mononuclear cells was lower than in PBMCs, ranging from a mean of 37.0 ± 21.4 to 105.8 ± 47.2 fmol/ 10^6 cells over the course of 70 days (fig. 5). As for FTC-TP, despite increasing nanochannel and reservoir size for this study, target preventative levels were not reached. Sustained levels of FTC-TP in PBMCs were detected from day 3 to day 28 (1223.7 ± 416.8 to 1656.7 ± 290.8 fmol/ 10^6 PBMCs), followed by a steady decline to 343.3 ± 102.9 fmol/ 10^6 PBMCs on day 70. In contrast to plasma FTC levels, the decreasing trend in FTC-TP PBMCs level was not observed until after day 28, possibly because of the longer intracellular FTC-TP half-life of 39 hours compared to 8–10 hours for plasma FTC (25). Similarly, FTC-TP levels in rectal mononuclear cells declined from a mean of 200.4 ± 104.4 fmol/ 10^6 cells on day 28 to below lower LOQ on day 70 (fig. 5).

3.5. Transcutaneous refilling of the NDIs to replenish reservoir

Because the consecutive decrease in FTC-TP concentrations after day 28 was likely due to drug exhaustion, transcutaneous refilling of all NDI implants was performed on day 70 to replenish the drug reservoir. As transcutaneous refilling of the NDI required drug in solution, we formulated a nanosuspension solution of FTC with Tween 80 and Pluronic F108 as surfactants, while TAF was solubilized with ethanol in PBS. FTC nanoformulation stability analyzed over 42 days via DLS showed that particle size changed from 387 nm with a zeta potential -37 mV to 256 nm with a zeta potential of -48 mV, indicating reasonable level of stability. The primary purpose of the formulations was to ensure syringeability and injectability of the drug for transcutaneous refilling of the NDI. On day 70, these TAF and FTC solutions were used to transcutaneously refill the reservoir through the ports (fig. 1D and fig. 6A). The ports were located by palpation of the skin, and a venting syringe was placed in the venting port to draw out excess drug, while drug-filled syringe was placed in the adjacent port to replenish drug reservoir as depicted in fig. 6B. In the scenario where the

ports are not palpable under the skin, ultrasonography can be performed to visualize the ports. To test this, we subcutaneously implanted an NDI in a pig cadaver and performed ultrasound to visualize the ports (fig. 6C). For this study, because the ports were palpable, ultrasound was not required for the transcutaneous refilling procedure. Based on the amount of residual drug retrieved from implants on day 70, we calculated average in vivo release rates of 1.7 mg/day for TAF and 41.8 mg/day for FTC (Table S2). While a comparable release rate (1.8 mg/day) was previously obtained for TAF during the pilot study (fig. S3), significantly higher values were achieved for FTC using 250 nm membranes, as compared to the pilot study with 20 nm channels (3.0 mg/day). By comparing in vitro and in vivo results, an increase of 8.1-fold in release was calculated for TAF, while a 15.7-fold increase was observed for FTC. Notably these data correlate well with TAF hydrophobicity and FTC hydrophilicity ($\log P$ at pH 7.4 = 2.24 and -0.73, respectively), and binding affinity to plasma proteins (80% and <3.6%, respectively) (46, 49). These results support our hypothesis that plasma molecules such as albumin, α 1-acid glycoprotein and lipoproteins may contribute to shuttle TAF from the NDI reservoir to the body.

3.6. TAF, TFV and FTC concentrations after transcutaneous refilling

Two days after transcutaneous drug refilling of the NDIs, plasma TAF, TFV, and FTC levels increased to 1.2 ± 1.1 , 10.5 ± 7.8 , and 507.3 ± 101.9 ng/ml respectively (fig. 3). Accordingly, analysis of PBMCs drug metabolite concentration demonstrated TFV-DP increased to a mean of 2490.0 ± 1295.5 fmol/ 10^6 cells, while FTC-TP levels increased to mean of 1557.0 ± 360.6 fmol/ 10^6 cells (fig. 4). While the increase in drug concentrations are indicative of successful refilling of the drug reservoirs, both TFV-DP and FTC-TP levels steadily declined two days after transcutaneous refilling (day 76, 78 and 83). We surmise that the decreased drug concentration could be attributed to the change from powder drug to drug in solution, which is lower in concentration and also could have encountered stability issues. At the end of study, rectal mononuclear TFV-DP levels reached a mean of 594.6 ± 569.2 fmol/ 10^6 cells whereas FTC-TP levels reached 731.6 ± 357.1 fmol/ 10^6 cells (fig. 5). We then evaluated TFV and FTC drug concentrations in anatomical sites associated with HIV infection where PrEP drug exposure is important, rectum, cheek pouch, cervix, and inguinal lymph nodes (LN), at the end of the study (fig. 7A). Our analysis revealed TFV and FTC exposure in the rectum, cheek pouch, cervix, and inguinal LN, indicating subcutaneous drug delivery from the NDI facilitated drug distribution to various HIV-associated anatomical compartments. We observed 8-fold lower TFV levels in the cervix in comparison to rectal tissue, consistent with literature reports of lower TFV drug exposure in female genital tissues (44, 50, 51). In contrast, FTC concentrations were consistently higher than TFV levels across all tissues, specifically 9-fold higher in the rectum, in accordance with previous studies (44, 51) and 22-fold higher in cervical tissue. Analysis of cervicovaginal fluid showed higher FTC concentrations across all time points compared to TFV, whereby TFV concentrations in the cervicovaginal fluid were detectable only on day 42 and 56 of the study (fig. 7B). While TFV and FTC were detected in the rectum and cheek pouch tissues at the end of the study, rectal and oral fluid samples collected concurrently with cervicovaginal fluid were below LOQ (data not shown) with the exception of FTC concentration in the rectal swabs on day 42 (55.8 ± 10.2 ng/ml).

3.7. Toxicity of NDI implantation and histological analysis of tissue surrounding implant.

All animals were healthy after device implantation. In the second study, one of three animals developed swelling around both NDI devices ten days post-implant. Pathology report on the serosanguineous fluid surrounding the implant showed elevated eosinophils, while complete blood count analysis demonstrated no systemic eosinophilia or signs of infection. This finding was consistent with seroma formation, which is commonly seen after implantation of medical devices (52, 53). The swelling resolved a week later, suggesting that the reaction was unlikely due to titanium allergy. Eight weeks after NDI implantation, one animal developed sterile dehiscence of the incision site over NDI-TAF. Surgery was performed to close the wound. On day 70, skin ulceration over NDI-TAF implants were revealed on two animals upon sterile scrubbing in preparation for transcutaneous refilling. Other than the aforementioned events, there were no additional significant abnormalities or notable toxicity issues. Histological analysis of punch biopsy of skin adjacent to NDI-TAF (fig. 8A) and NDI-FTC (fig. 8B) implant showed normal skin morphology. At the end of the study, there was minimal inflammation in the fibrotic capsule of NDI-TAF (fig. 8C), despite the aforementioned issue of dehiscence of the incision site in two animals. Conversely, histological analysis of fibrotic capsules surrounding the NDI-FTC displayed some immune cell infiltration on the surface adjacent to the drug-releasing side of the NDI on two animals (fig. 8D). As this reaction was not observed in the pilot study, it is plausible that the reaction could be attributed to the nanosuspension formulation of FTC used for reservoir refilling. SEM analysis of the membrane retrieved from NDI-PBS showed minimal channel occlusion after 60 days of implantation (fig. 8E), confirming that channels remain unobstructed.

4. DISCUSSION

TFV and FTC are effective at conferring protection from HIV transmission when adhered to daily dosing regimen. However, adherence remains an obstacle for effective HIV PrEP. Here we developed a sustained drug delivery implant for long-term release of TAF and FTC for HIV PrEP to overcome adherence challenges. We utilized TAF in our study due to its potent antiviral activity at 25 to 30-fold lower dose (10–25 mg) than TDF (300 mg). A 25 mg dose of TAF resulted in 5 times more intracellular TFV-DP and reduced systemic TFV exposure, when compared to a 300 mg TDF dose (54). Though both TAF and TDF have similar HIV resistance profile, TAF has a higher inhibitory quotient and its resulting TFV-DP concentration in PBMCs diminishes the risk of developing resistance throughout the course of PrEP (55, 56). Evidently, superior antiviral efficacy is achieved with low doses of TAF, thus allowing for compatibility in long-term drug delivery systems. While TAF and FTC are conventionally administered orally, research demonstrates comparable efficacy of subcutaneous TAF and FTC administration (24, 51, 57). A study of subdermal implant for long-term TAF delivery in beagle dogs indicated that subcutaneous doses as low as 0.15 mg/day may be sufficient to maintain effective concentrations of TFV-DP in PBMCs (24). Further, daily subcutaneous injections of FTC (20 mg/kg) and TFV (22 mg/kg) were demonstrated to protect against rectally transmitted SHIV in rhesus macaques (57). Here we showed that subcutaneous TAF and FTC delivery via the NDI was achieved in rhesus macaques for more than two months, validating the use of the NDI as an effective drug delivery platform for HIV PrEP.

As TFV-DP and FTC-TP concentrations in PBMCs are clinically accepted parameters for approximating threshold protective drug levels, we primarily focused on these active drug metabolites to determine the achievable drug concentrations via NDI-mediated drug delivery in rhesus macaques. We reported that subcutaneous delivery of TAF via the NDI was able to maintain TFV-DP PBMCs levels up to 12 times more than the preventative target of 40 fmol/10⁶ cells over the course of 83 days. This suggests that sustained delivery via the NDI could allow for dose reduction of TAF. The long-lasting intracellular TFV-DP levels observed in rhesus macaques in our study were akin to levels seen in clinical studies, whereby average intracellular TFV-DP concentration ranged from 80 to 160 fmol/10⁶ cells (25, 58). Based on the increasing TFV-DP concentration in PBMCs over 70 days before drug refilling, it is conceivable that TAF release via the NDI could be sustained above preventative target concentration without transcutaneous refilling for at least six months. Preventative levels of FTC-TP were not achieved in our study, likely due to the high dosage required of FTC, which presents a significant limitation for drug delivery implants. An important factor for protection against HIV is sufficient drug distribution to tissues relevant for viral transmission. We demonstrated varying but sustained levels of TAF, TFV and FTC in plasma and TFV-DP and FTC-TP exposure in rectal mononuclear cells (with the exception of FTC-TP on day 70) throughout the duration of study. Our results showed TFV and FTC drug penetration in the rectum, cheek pouch, cervix, and inguinal LN (fig. 7B), further validating effective drug distribution from subcutaneous delivery via the NDI.

Existing drug-eluting systems have a finite depot and lack methods for refilling upon payload exhaustion. We reported here a minimally invasive procedure to transcutaneously refill the NDI without device explantation, thereby extending the release duration of ARVs. This extension of drug release duration allows for the implants to potentially be utilized for many years. Drug loading ports in the NDIs were palpable under the skin in this study, allowing for transcutaneous refilling without requiring additional imaging technology to locate the ports. Considering the scenario that the ports may not be palpable, the ports can be visualized via ultrasound imaging, which is widely used in developed countries and a more accessible type of imaging modality in developing countries. After the transcutaneous refilling procedure, we observed increase in plasma TAF, TFV and FTC levels, along with rise in TFV-DP and FTC-TP levels in PBMCs and rectal mononuclear cells. The transient spike observed in TFV-DP and FTC-TP concentrations in PBMCs on day 72 could be attributed to the change from powder drug to drug in a liquid solution for transcutaneous refilling. The NDI implant was loaded with powder drug before implantation, which required dissolution in PBS (during priming of the device prior to implantation) and in physiological fluids (after implantation) over time before being released from the nanochannels. Because solubilized drug was used for transcutaneous refilling, it is possible that faster release from the NDI occurred, resulting in a spike in PBMCs concentration of TFV-DP and FTC-TP on day 72. The steep decline of TFV-DP levels observed two days after transcutaneous refilling was conceivably due to stability issues from the TAF drug formulation in solution. Similarly, we detected that FTC-TP levels gradually decreased two days after transcutaneous refilling, also potentially due to drug stability. As such, extensive formulation studies are required to improve drug stability in solution.

Our study showed that the NDI could be an effective approach for delivering TAF-based HIV PrEP, as indicated by the clinically relevant TFV-DP concentration in PBMCs and drug exposure in tissues relevant to HIV transmission. This is relevant as PrEP with TDF alone was effective in sero-discordant couples (4). While our results are encouraging, the study is not without limitations. Despite efforts to augment FTC levels by increasing reservoir and nanochannel size in our second study, the failure to achieve clinically-relevant preventative target portend the limitations of subcutaneous delivery of FTC via the implants. Although FTC is a broadly used ARV in dual drug combination strategies for HIV treatment and prevention, a major disadvantage is the large volume distribution required and short plasma half-life of 8 to 10 hours, which necessitates a high daily dosage (47). Because of this, the drug reservoir for FTC would need to be substantially larger, in addition to adoption of a membrane housing at least three times the number of nanochannels to achieve the desired dose. As such, the size required of the device for effective delivery of FTC itself as an active pharmaceutical ingredient without further formulation development would be impractical for subcutaneous implants. Numerous research groups are currently exploring approaches to extend FTC plasma half-life, such as investigation of nanocarrier-based formulations to enhance FTC loading and prolong intracellular FTC concentration (47). In the second study, we encountered an issue with wound dehiscence over the smaller implant, NDI-TAF, which could be attributed to the age of the animals. As this occurred in the two geriatric animals, and not the younger animal, it is also possible that the implant design created a tension under the skin of the older animals, which is less elastic. This is an additional parameter to consider for subcutaneous implant design and procedures. Further, additional studies are needed to validate the preventive efficacy of the NDI-facilitated PrEP delivery using simian HIV challenge models. The clinical translation value of the NDI as a PrEP drug delivery system could be improved with a more potent formulation of FTC and with a dual chamber depot in a single device. Moreover, we are currently developing a refined drug delivery implant that can be controlled remotely via Bluetooth to tune the release of drugs via modulation of an applied electrical field to the nanochannel membrane as well as a safety mechanism for ceasing drug release via an external magnetic field (59–61).

5. CONCLUSIONS

Overall, our data establishes the NDI implant as an effective drug delivery approach to overcome one of the key obstacles in HIV prevention - adherence to daily dosing regimens. Sustained release of ARVs via the NDI implant could eliminate PrEP drug adherence issues and tailor to the needs of populations with limited access to PrEP drugs, such as adolescents and people at risk of HIV infection living in low-income countries (62–64). Further, the transcutaneous refillable feature of the NDI represents an innovative approach to extend the duration of PrEP drug delivery, which is a significant limitation of conventional long-acting drug implants such as polymer pellets, osmotic pumps, and vaginal rings (23). This implantable drug delivery device offers the convenience of user-independence, biocompatibility, and refillability without explantation, which could increase the acceptance rate for implantable devices. Greene et. al demonstrated in a cohort of MSM, the acceptance rate of non-visible implants was markedly higher than injections or visible implants (34.3% versus 25.2% and 4.3%, respectively) (65). Moreover, the opportunity to extend the dosing

interval from 1 week to 3 months with long-acting injectables, or to 12 month for a refillable implant would be advantageous to reduce the risk of patient non-adherence to PrEP (66). A straightforward refilling procedure would also reduce the stress to the patient and the injection site reactions, which have been relevant in the phase 2 studies of long-acting ARVs such as cabotegravir and rilpivirine (67). Most importantly, the broad drug compatibility of the NDI device could be extended for delivery of other HIV PrEP treatment regimens or other drugs for different clinical indications. In a large scale fabrication setting, all implant components including the nanochannel membrane, could be produced inexpensively, to the extent that this technology could be promising for deployment in underdeveloped countries. In this context, both sustained release and transcutaneous refilling capabilities could be key in addressing the need of patients with limited access to medical services as well as adherence issues.

Supplementary Material

Refer to Web version on PubMed Central for supplementary material.

ACKNOWLEDGEMENTS

We thank Carlos Favela and Dr. Kemi Cui from the advanced cellular and tissue microscopy core, Dr. Jianhua “James” Gu from the electron microscopy core, Dr. Andreana L. Rivera, Dr. Yulan Ren, and Sandra Steptoe from the research pathology core of Houston Methodist Research Institute. We express our gratitude to Trevor Hawkins and Jim Rooney at Gilead for their support and fruitful discussions. We thank Luke Segura, Elizabeth Lindemann, Dr. Greg Wilkerson from the Michale E. Keeling Center for Comparative medicine and Research at UTMDACC for support in animal studies. TAF and FTC were provided by Gilead Sciences

Funding

This work was supported by NIH R01 AI120749–01A1 and start-up funds from Houston Methodist Research Institute (AG).

REFERENCES

1. UNAIDS, “Global AIDS update 2016,” (Joint United Nations Programme on HIV/AIDS, Geneva, Switzerland, 2016).
2. “Prevention gap report,” (Joint United Nations Programme on HIV/AIDS, 2016).
3. Kojima N, Klausner JD, Is Emtricitabine-Tenofovir Disoproxil Fumarate Pre-exposure Prophylaxis for the Prevention of Human Immunodeficiency Virus Infection Safer Than Aspirin? *Open Forum Infect Dis* 3, ofv221 (2016). [PubMed: 26949714]
4. Baeten JM et al., Antiretroviral prophylaxis for HIV prevention in heterosexual men and women. *N Engl J Med* 367, 399–410 (2012). [PubMed: 22784037]
5. Thigpen MC et al., Antiretroviral preexposure prophylaxis for heterosexual HIV transmission in Botswana. *N Engl J Med* 367, 423–434 (2012). [PubMed: 22784038]
6. Grant RM et al., Preexposure chemoprophylaxis for HIV prevention in men who have sex with men. *N Engl J Med* 363, 2587–2599 (2010). [PubMed: 21091279]
7. McCormack S et al., Pre-exposure prophylaxis to prevent the acquisition of HIV-1 infection (PROUD): effectiveness results from the pilot phase of a pragmatic open-label randomised trial. *Lancet* 387, 53–60 (2016). [PubMed: 26364263]
8. Molina JM et al., On-Demand Preexposure Prophylaxis in Men at High Risk for HIV-1 Infection. *N Engl J Med* 373, 2237–2246 (2015). [PubMed: 26624850]
9. Gengiah TN, Moosa A, Naidoo A, Mansoor LE, Adherence challenges with drugs for pre-exposure prophylaxis to prevent HIV infection. *Int J Clin Pharm* 36, 70–85 (2014). [PubMed: 24129582]

10. Grant RM et al., Uptake of pre-exposure prophylaxis, sexual practices, and HIV incidence in men and transgender women who have sex with men: a cohort study. *Lancet Infect Dis* 14, 820–829 (2014). [PubMed: 25065857]
11. Anderson PL et al., Emtricitabine-tenofovir concentrations and pre-exposure prophylaxis efficacy in men who have sex with men. *Sci Transl Med* 4, 151ra125 (2012).
12. UNAIDS, “Prevention Gap Report,” (Joint United Nations Programme on HIV/AIDS, Geneva, Switzerland, 2016).
13. McGowan I et al., A Phase 1 Randomized, Open Label, Rectal Safety, Acceptability, Pharmacokinetic, and Pharmacodynamic Study of Three Formulations of Tenofovir 1% Gel (the CHARM-01 Study). *PLoS One* 10, e0125363 (2015). [PubMed: 25942472]
14. Pines HA et al., Acceptability of potential rectal microbicide delivery systems for HIV prevention: a randomized crossover trial. *AIDS Behav* 17, 1002–1015 (2013). [PubMed: 23114512]
15. Malcolm RK et al., Pharmacokinetics and efficacy of a vaginally administered maraviroc gel in rhesus macaques. *J Antimicrob Chemother* 68, 678–683 (2013). [PubMed: 23111849]
16. Moss JA et al., Combination Pod-Intravaginal Ring Delivers Antiretroviral Agents for HIV Prophylaxis: Pharmacokinetic Evaluation in an Ovine Model. *Antimicrob Agents Chemother* 60, 3759–3766 (2016). [PubMed: 27067321]
17. Zhao C et al., Pharmacokinetics and Preliminary Safety of Pod-Intravaginal Rings Delivering the Monoclonal Antibody VRC01-N for HIV Prophylaxis in a Macaque Model. *Antimicrob Agents Chemother*, (2017).
18. Smith JM et al., Intravaginal ring eluting tenofovir disoproxil fumarate completely protects macaques from multiple vaginal simian-HIV challenges. *Proc Natl Acad Sci U S A* 110, 16145–16150 (2013). [PubMed: 24043812]
19. Clark JT et al., Engineering a segmented dual-reservoir polyurethane intravaginal ring for simultaneous prevention of HIV transmission and unwanted pregnancy. *PLoS One* 9, e88509 (2014). [PubMed: 24599325]
20. Murphy DJ et al., Pre-clinical development of a combination microbicide vaginal ring containing dapivirine and darunavir. *J Antimicrob Chemother* 69, 2477–2488 (2014). [PubMed: 24862093]
21. Nel A et al., Safety and Efficacy of a Dapivirine Vaginal Ring for HIV Prevention in Women. *N Engl J Med* 375, 2133–2143 (2016). [PubMed: 27959766]
22. Gorbach PM et al., Order of orifices: sequence of condom use and ejaculation by orifice during anal intercourse among women: implications for HIV transmission. *J Acquir Immune Defic Syndr* 67, 424–429 (2014). [PubMed: 25356778]
23. Schlesinger E et al., A Tunable, Biodegradable, Thin-Film Polymer Device as a Long-Acting Implant Delivering Tenofovir Alafenamide Fumarate for HIV Pre-exposure Prophylaxis. *Pharm Res* 33, 1649–1656 (2016). [PubMed: 26975357]
24. Gunawardana M et al., Pharmacokinetics of long-acting tenofovir alafenamide (GS7340) subdermal implant for HIV prophylaxis. *Antimicrob Agents Chemother* 59, 3913–3919 (2015). [PubMed: 25896688]
25. Anderson PL et al., Pharmacological considerations for tenofovir and emtricitabine to prevent HIV infection. *J Antimicrob Chemother* 66, 240–250 (2011). [PubMed: 21118913]
26. Sax PE et al., Tenofovir alafenamide vs. tenofovir disoproxil fumarate in single tablet regimens for initial HIV-1 therapy: a randomized phase 2 study. *J Acquir Immune Defic Syndr* 67, 52–58 (2014). [PubMed: 24872136]
27. Anderson PL, Glidden DV, Bushman LR, Heneine W, Garcia-Lerma JG, Tenofovir diphosphate concentrations and prophylactic effect in a macaque model of rectal simian HIV transmission. *J Antimicrob Chemother* 69, 2470–2476 (2014). [PubMed: 24862094]
28. Ferrati S et al., Leveraging nanochannels for universal, zero-order drug delivery in vivo. *J Control Release* 172, 1011–1019 (2013). [PubMed: 24095805]
29. Fine D et al., A robust nanofluidic membrane with tunable zero-order release for implantable dose specific drug delivery. *Lab Chip* 10, 3074–3083 (2010). [PubMed: 20697650]
30. Bruno G et al., Unexpected behaviors in molecular transport through size-controlled nanochannels down to the ultra-nanoscale. *Nat Commun* 9, 1682 (2018). [PubMed: 29703954]

31. Geninatti TS, E.; Grattoni A, Robotic UV-Vis apparatus for long-term characterization of drug release from nanochannels. *Measurement Science and Technology* 25, (2014).
32. Hendrix CW et al., Dose Frequency Ranging Pharmacokinetic Study of Tenofovir-Emtricitabine After Directly Observed Dosing in Healthy Volunteers to Establish Adherence Benchmarks (HPTN 066). *AIDS Res Hum Retroviruses* 32, 32–43 (2016). [PubMed: 26414912]
33. Herold BC et al., Antiviral activity of genital tract secretions after oral or topical tenofovir pre-exposure prophylaxis for HIV-1. *J Acquir Immune Defic Syndr* 66, 65–73 (2014). [PubMed: 24457633]
34. Bushman LR et al., Determination of nucleoside analog mono-, di-, and tri-phosphates in cellular matrix by solid phase extraction and ultra-sensitive LC-MS/MS detection. *J Pharm Biomed Anal* 56, 390–401 (2011). [PubMed: 21715120]
35. Seifert SM et al., Intracellular Tenofovir and Emtricitabine Anabolites in Genital, Rectal, and Blood Compartments from First Dose to Steady State. *AIDS Res Hum Retroviruses* 32, 981–991 (2016). [PubMed: 27526873]
36. Ferrati S et al., The nanochannel delivery system for constant testosterone replacement therapy. *J Sex Med* 12, 1375–1380 (2015). [PubMed: 25930087]
37. Filgueira CS et al., Sustained zero-order delivery of GC-1 from a nanochannel membrane device alleviates metabolic syndrome. *Int J Obes (Lond)* 40, 1776–1783 (2016). [PubMed: 27460601]
38. Filgueira CS et al., A pharmacokinetic study of GC-1 delivery using a nanochannel membrane device. *Nanomedicine* 13, 1739–1744 (2017). [PubMed: 28259802]
39. Pimpinelli A, Ferrari M, and Grattoni Alessandro, Scaling and crossovers in molecular transport in nano-fluidic systems. *Applied Physics Letters* 103, 113104 (2013).
40. Grattoni A et al., Gated and near-surface diffusion of charged fullerenes in nanochannels. *ACS Nano* 5, 9382–9391 (2011). [PubMed: 22032773]
41. Colas J. C. a. A., in *Biomaterials Science*, Buddy ASH Ratner D, Schoen Frederick J., Lemons Jack E., Ed. (Academic Press, New York, 2004), chap. Application of materials in medicine, biology, and artificial organs, pp. 697–707.
42. Voskerician G et al., Biocompatibility and biofouling of MEMS drug delivery devices. *Biomaterials* 24, 1959–1967 (2003). [PubMed: 12615486]
43. Williams DF, *Titanium for Medical Applications Titanium in Medicine: Material Science, Surface Science, Engineering* (Springer-Verlag Berlin Heidelberg, New York, 2001).
44. Patterson KB et al., Penetration of tenofovir and emtricitabine in mucosal tissues: implications for prevention of HIV-1 transmission. *Sci Transl Med* 3, 112re114 (2011).
45. Ferrati S et al., Delivering enhanced testosterone replacement therapy through nanochannels. *Adv Healthc Mater* 4, 446–451 (2015). [PubMed: 25274059]
46. Custodio JM et al., Pharmacokinetics and Safety of Tenofovir Alafenamide in HIV-Uninfected Subjects with Severe Renal Impairment. *Antimicrob Agents Chemother* 60, 5135–5140 (2016). [PubMed: 27216057]
47. Mandal S, Belshan M, Holec A, Zhou Y, Destache CJ, An Enhanced Emtricitabine-Loaded Long-Acting Nanoformulation for Prevention or Treatment of HIV Infection. *Antimicrob Agents Chemother* 61, (2017).
48. Seifert SM et al., Dose response for starting and stopping HIV preexposure prophylaxis for men who have sex with men. *Clin Infect Dis* 60, 804–810 (2015). [PubMed: 25409469]
49. de Lastours V, Fonsart J, Burlacu R, Gourmel B, Molina JM, Concentrations of tenofovir and emtricitabine in saliva: implications for preexposure prophylaxis of oral HIV acquisition. *Antimicrob Agents Chemother* 55, 4905–4907 (2011). [PubMed: 21788466]
50. Radzio J et al., Prevention of vaginal SHIV transmission in macaques by a coitally-dependent Truvada regimen. *PLoS One* 7, e50632 (2012). [PubMed: 23226529]
51. Garcia-Lerma JG et al., Intermittent prophylaxis with oral Truvada protects macaques from rectal SHIV infection. *Sci Transl Med* 2, 14ra14 (2010).
52. Knight KH, Brand FM, McHaourab AS, Veneziano G, Implantable intrathecal pumps for chronic pain: highlights and updates. *Croat Med J* 48, 22–34 (2007). [PubMed: 17309136]

53. Renard E et al., Implantable insulin pumps: infections most likely due to seeding from skin flora determine severe outcomes of pump-pocket seromas. *Diabetes Metab* 27, 62–65 (2001). [PubMed: 11240448]
54. Ruane PJ et al., Antiviral activity, safety, and pharmacokinetics/pharmacodynamics of tenofovir alafenamide as 10-day monotherapy in HIV-1-positive adults. *J Acquir Immune Defic Syndr* 63, 449–455 (2013). [PubMed: 23807155]
55. Margot NA, Johnson A, Miller MD, Callebaut C, Characterization of HIV-1 Resistance to Tenofovir Alafenamide In Vitro. *Antimicrob Agents Chemother* 59, 5917–5924 (2015). [PubMed: 26149983]
56. Margot NA, Liu Y, Miller MD, Callebaut C, High resistance barrier to tenofovir alafenamide is driven by higher loading of tenofovir diphosphate into target cells compared to tenofovir disoproxil fumarate. *Antiviral Res* 132, 50–58 (2016). [PubMed: 27208653]
57. Garcia-Lerma JG et al., Prevention of rectal SHIV transmission in macaques by daily or intermittent prophylaxis with emtricitabine and tenofovir. *PLoS Med* 5, e28 (2008). [PubMed: 18254653]
58. Hawkins T et al., Intracellular pharmacokinetics of tenofovir diphosphate, carbovir triphosphate, and lamivudine triphosphate in patients receiving triple-nucleoside regimens. *J Acquir Immune Defic Syndr* 39, 406–411 (2005). [PubMed: 16010161]
59. Farina M et al., Remote magnetic switch off microgate for nanofluidic drug delivery implants. *Biomed Microdevices* 19, 42 (2017). [PubMed: 28484917]
60. Bruno G et al., Leveraging electrokinetics for the active control of dendritic fullerene-1 release across a nanochannel membrane. *Nanoscale* 7, 5240–5248 (2015). [PubMed: 25707848]
61. Bruno G et al., The active modulation of drug release by an ionic field effect transistor for an ultra-low power implantable nanofluidic system. *Nanoscale* 8, 18718–18725 (2016). [PubMed: 27787528]
62. Krakower DS, Mayer KH, Pre-exposure prophylaxis to prevent HIV infection: current status, future opportunities and challenges. *Drugs* 75, 243–251 (2015). [PubMed: 25673022]
63. Hosek S et al., Preventing HIV among adolescents with oral PrEP: observations and challenges in the United States and South Africa. *J Int AIDS Soc* 19, 21107 (2016). [PubMed: 27760684]
64. Haire B, Kaldor JM, Ethics of ARV based prevention: treatment-as-prevention and PrEP. *Dev World Bioeth* 13, 63–69 (2013). [PubMed: 23594312]
65. Greene GJ et al., Preferences for Long-Acting Pre-exposure Prophylaxis (PrEP), Daily Oral PrEP, or Condoms for HIV Prevention Among U.S. Men Who Have Sex with Men. *AIDS Behav* 21, 1336–1349 (2017). [PubMed: 27770215]
66. Owen A, Rannard S, Strengths, weaknesses, opportunities and challenges for long acting injectable therapies: Insights for applications in HIV therapy. *Adv Drug Deliv Rev* 103, 144–156 (2016). [PubMed: 26916628]
67. Landovitz RJ, Kofron R, McCauley M, The promise and pitfalls of long-acting injectable agents for HIV prevention. *Curr Opin HIV AIDS* 11, 122–128 (2016). [PubMed: 26633643]

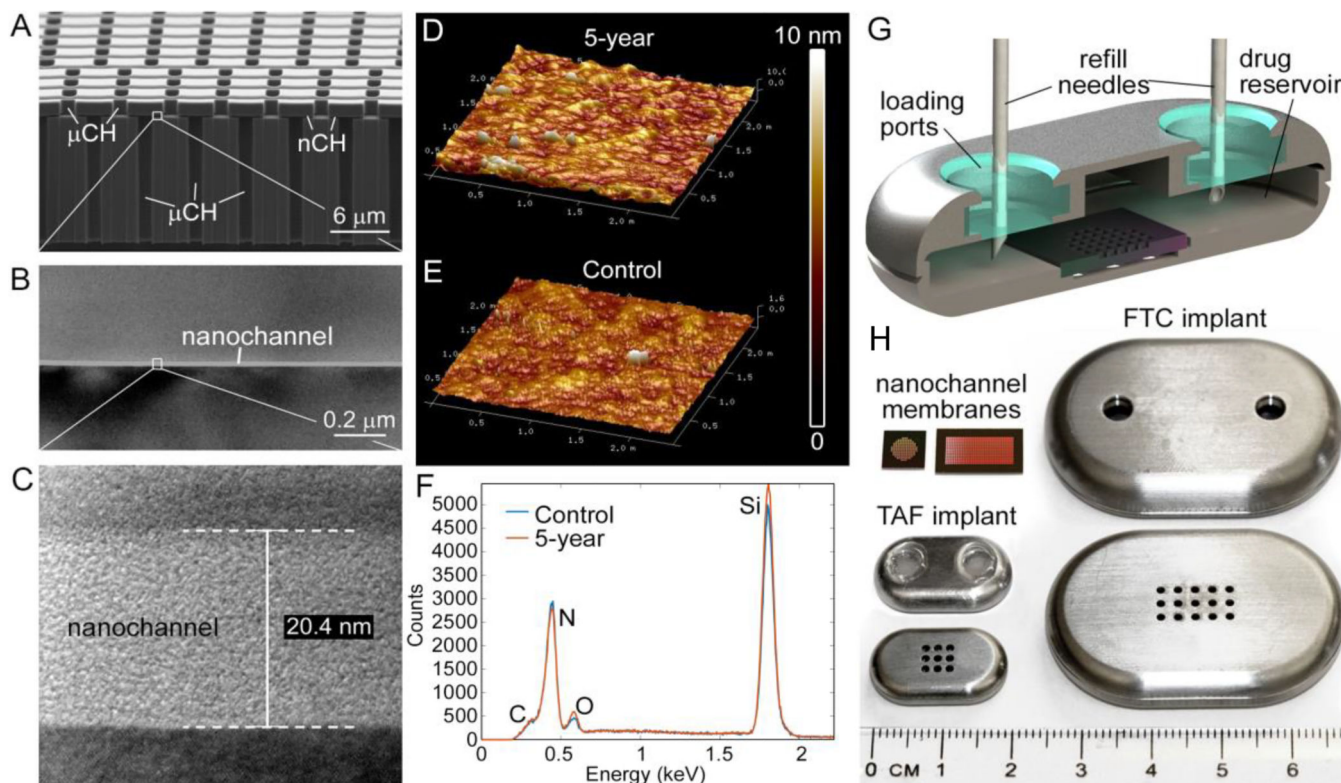


Figure 1. Nanochannel membrane and NDI.

(A) Scanning electron microscopic image of nanochannel (nCH) membrane with microchannels (μ CH). (B), (C) Transmission electron microscopic image depicting 20 nm nanochannel. (D) Representative AFM image of membrane in PBS at 23 °C over 5 years compared to (E) fresh membrane. (F) EDX analysis of surface elements below TaN/SiC coating of membrane in PBS at 23 °C over 5 years compared to fresh control. (G) Cross-sectional rendering of NDI depicting drug refill needles through the loading ports with resealable silicon plugs. (H) Nanochannel membranes of two different sizes, square (TAF) and rectangle (FTC); top and bottom view of NDI in medical-grade titanium for TAF (with silicon plug) and FTC (before affixing silicon plug).

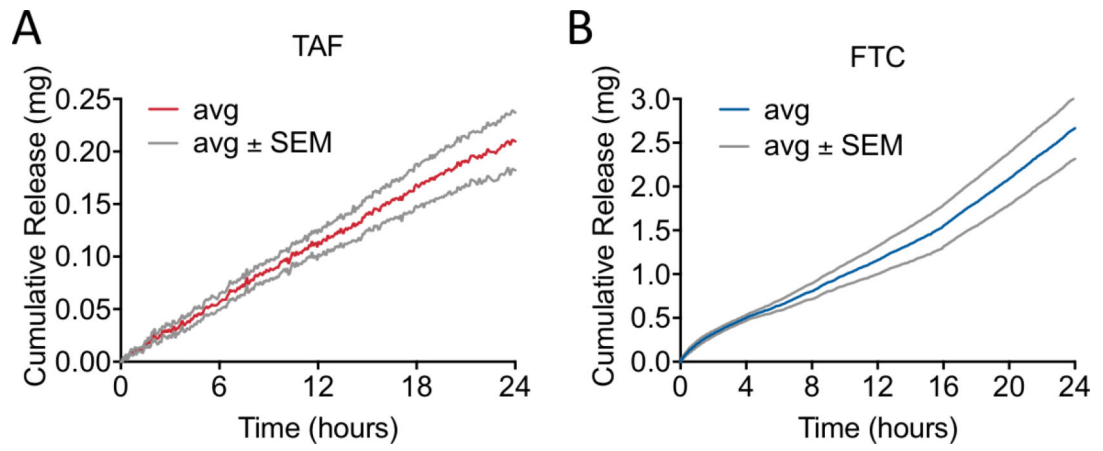


Figure 2. *In vitro* cumulative release of TAF or FTC.

NDI with 20 nm nanochannel membranes for (A) TAF (n = 4) and (B) FTC (n = 4) over 24 hours. Data show average (avg) values \pm SEM.

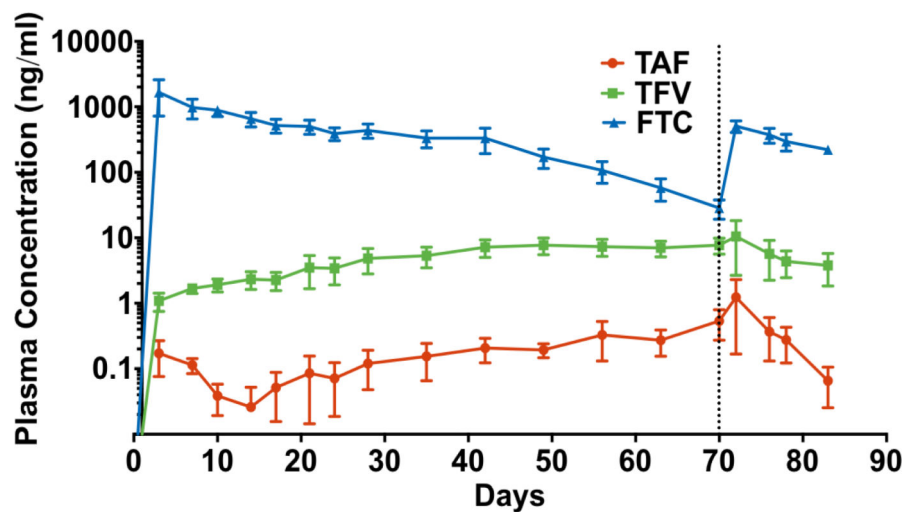


Figure 3. Pharmacokinetic profile of TAF, TFV and FTC plasma levels in rhesus macaques. Plasma drug concentrations of TAF (red), TFV (green) and FTC (blue) were analyzed at indicated time points via LC-MS/MS. Vertical dotted line marks day of transcutaneous refilling of NDI-TAF and NDI-FTC devices. Data points represent mean \pm SEM ($n = 3$).

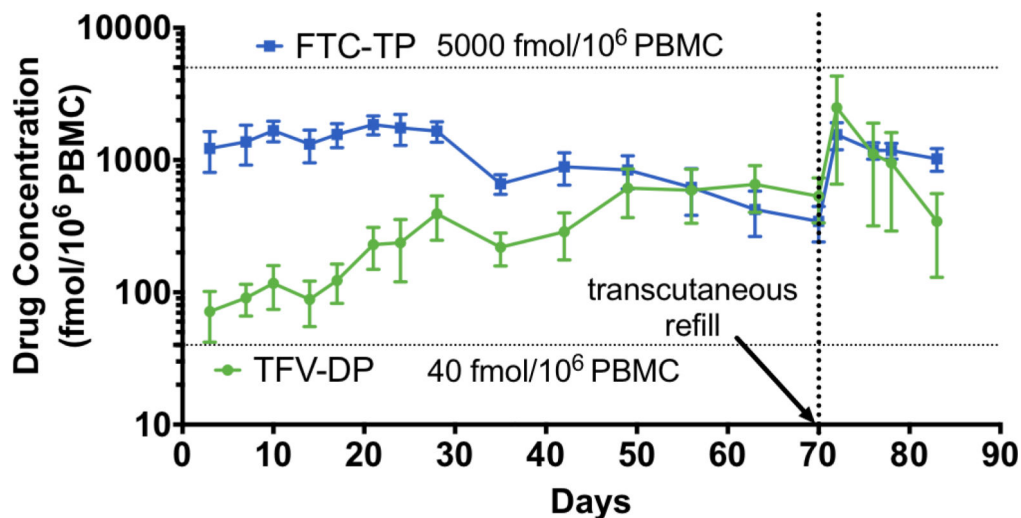


Figure 4. Pharmacokinetic profile of TFV-DP and FTC-TP in PBMCs.

Concentrations of TFV-DP (green) and FTC-TP (blue) in PBMCs from three rhesus macaques at the indicated time points analyzed by LC-MS/MS. Data points represent mean \pm SEM. Horizontal dotted line represents preventative target concentration for effective PrEP. Vertical dotted line represents day of transcutaneous refilling of NDI implants (day 70). Animals were euthanized on day 83.

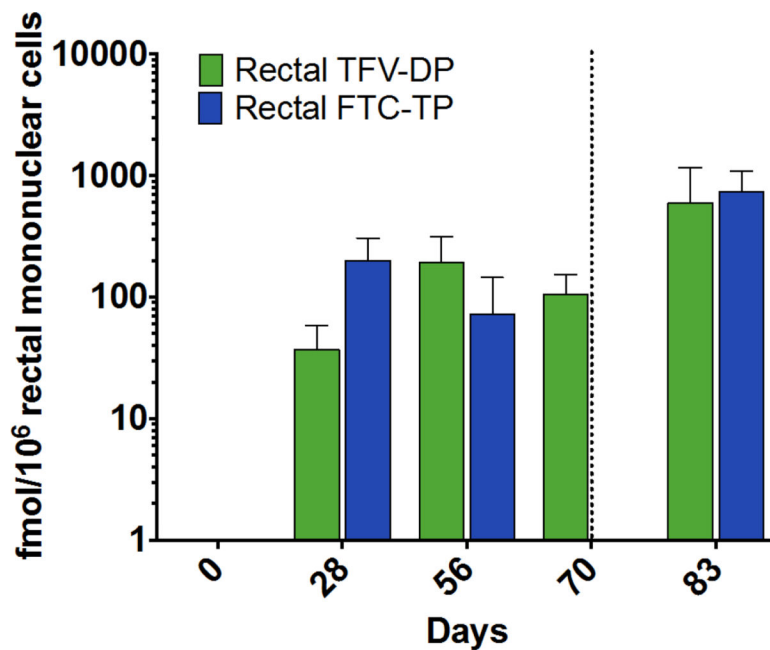


Figure 5. TFV-DP and FTC-TP concentrations in rectal mononuclear cells.

TFV-DP (green) and FTC-TP (blue) levels in rectal mononuclear cells from three rhesus macaques measured using LC-MS/MS. Each data point represents the means \pm SEM and vertical dotted lines correspond to the day of transcutaneous refilling of NDI reservoirs (day 70).

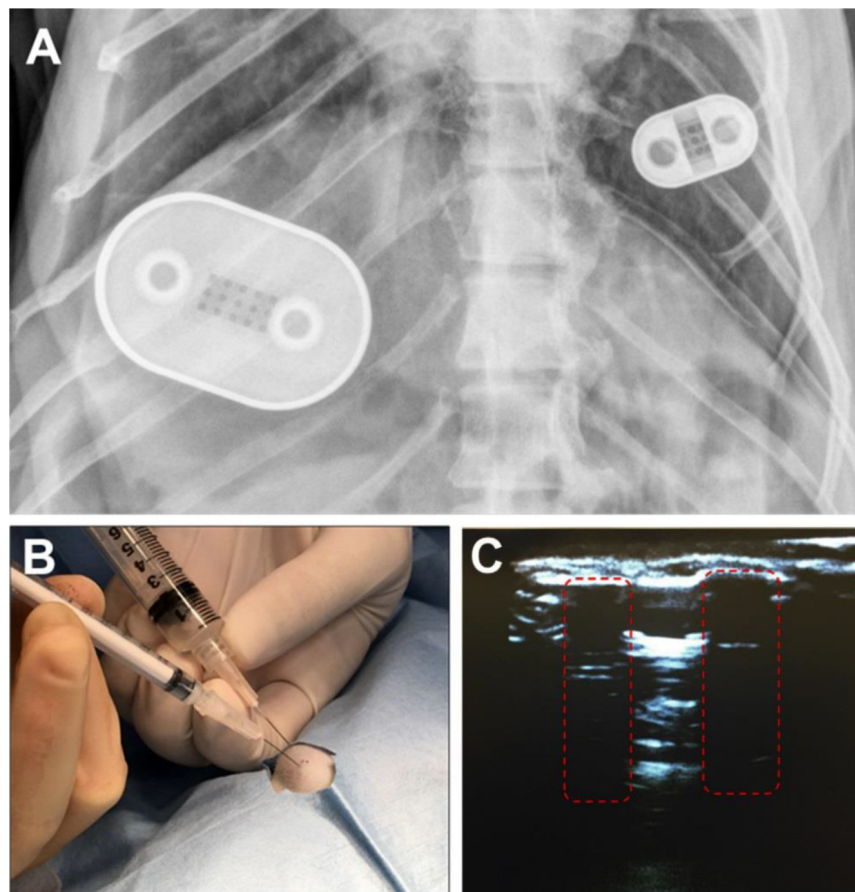


Figure 6. NDI implants in rhesus macaque on day 49 and transcutaneous drug refilling. (A) X-ray radiography image on day 49 of NDI-FTC (left) and NDI-TAF (right) implanted subcutaneously in the dorsum of a rhesus macaque. During surgical implantation of the NDIs, the side with drug refilling ports was positioned up and drug-eluting side with nanochannel membrane facing down. (B) Transcutaneous refilling procedure of NDI-TAF in the dorsum of a rhesus macaque. A venting syringe was inserted into one port, while a drug solution-filled syringe was inserted into the other port. Injection of drug was performed simultaneous to the withdrawal of residual fluid through the venting syringe. (C) Ultrasound image of loading and venting ports (red dashed boxes) of NDI-FTC subcutaneously implanted in a pig cadaver.

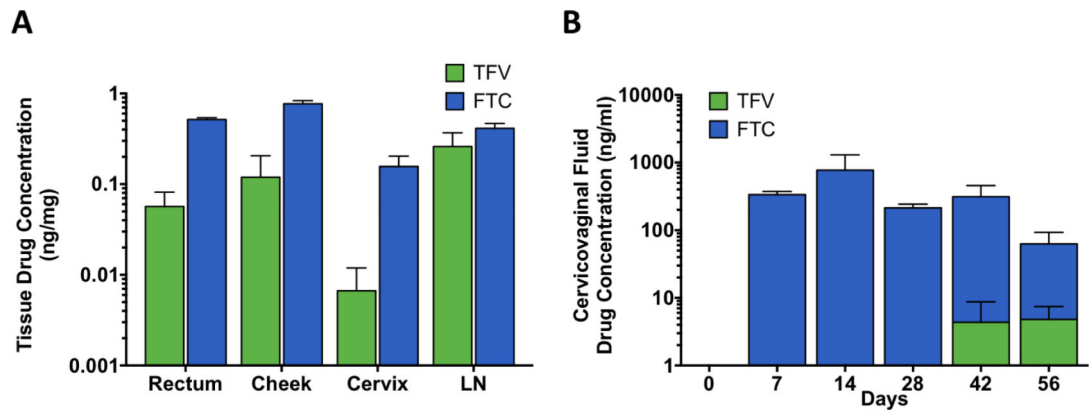


Figure 7. TFV and FTC concentration in tissues and cervicovaginal fluid.

LC-MS/MS analysis of (A) rectum, cheek, inguinal lymph node (LN) and cheek pouch at study termination (day 83) and (B) cervicovaginal fluid at indicated time points from three rhesus macaques. Data represent the means \pm SEM.

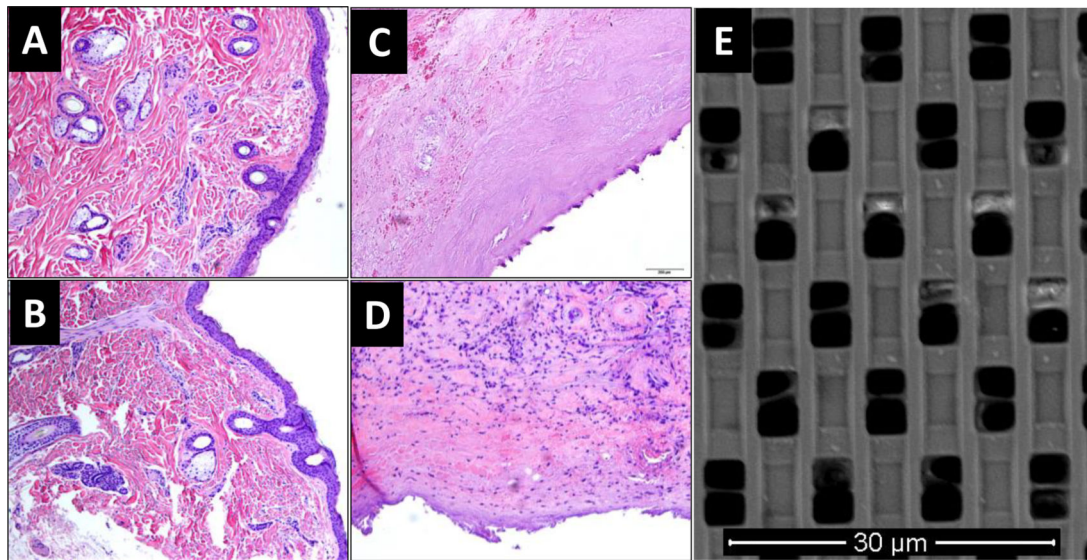


Figure 8. Histology of tissue samples and SEM image of nanochannel membrane.

Skin biopsy adjacent to (A) NDI-TAF and (B) NDI-FTC on day 30. Fibrotic capsule surrounding (C) NDI-TAF and (D) NDI-FTC at the end of the study (day 83). (E) Scanning electron microscopy image of nanochannel membrane retrieved from rhesus macaque in pilot study after 60 days of implantation.